Thermochimica Acta, 191 (1991) 161–178
Elsevier Science Publishers B.V., Amsterdam

Thermal decomposition of wood in oxidizing atmosphere. A kinetic study from non-isothermal TG experiments

T. Cordero, J.M. Rodríguez-Maroto, F. García and J.J. Rodríguez [1]
Department of Chemical Engineering, University of Málaga, 29071 Málaga (Spain)
(Received 25 March 1991)

Abstract

The kinetics of thermal decomposition of four wood species in oxygen-bearing atmospheres of 5, 10 and 20% molar O_2 concentrations have been studied from temperature-programmed experiments carried out at 5, 10 and 20 K min^{-1} heating rate. Devolatilization as well as combustion of the reamining solid have been considered to analyze the weight loss curves. The homogeneous volume reaction (VR) model has been used to describe devolatilization, whereas for solid combustion the grain model has been also checked. A two-stage approach has been used to fit the conversion–time curves and to derive the corresponding apparent kinetic parameters. The VR/VR (pyrolysis/combustion) combination provided a better description of the experimental $\alpha-t$ curves than the VR/grain combination. Holm oak and cork oak showed very close reactivities, whereas some differences were observed for aleppo pine and eucalyptus.

INTRODUCTION

A correct design of pyrolysis, gasification and controlled combustion systems for lignocellulosic biomass requires the knowledge of the corresponding gas–solid reaction kinetics under defined operating conditions such as temperature range, thermal regime, particle size and gas atmosphere.

In spite of the chemical heterogeneity of a raw material, its thermal decomposition under inert or reactive atmospheres can be described from an overall standpoint by following the weight loss of the solid sample. Isothermal and dynamic (temperature-programmed) thermogravimetric experiments have commonly been used to investigate the reactivities of carbonaceous materials such as wood [1–3], coal [4,5] and chars [4–11] in oxidizing atmospheres. For raw materials having a high volatile matter content, like wood and low-rank coals, dynamic TG runs starting from low temperature are necessary because isothermal operation leaves uncovered a substantial amount of the initial conversion region unless special arrangements are used.

[1] Author to whom correspondence should be addressed.

The higher the desired temperature, the more significant this problem will be.

Several kinetic expressions corresponding to different well known models have been proposed in the literature to describe the kinetics of non-catalytic gas–solid reactions. An interesting review was presented by Ramachandran and Doraiswamy [12]. In this work we will check two of them: the homogeneous volume reaction (VR) model and the grain model. We have not included in our study models accounting for changes in porosity and surface area occurring upon reaction [13–17]; such models have been mainly applied to gasification of microporous chars, where a substantial accessible internal surface area is initially present, which is not the case with wood.

In our previous work [18] we have studied the kinetics of holm oak wood pyrolysis from dynamic and isothermal TG experiments. A number of different existing models was checked. In each case, the VR model was always the best-fitting one, so we will use it to describe the devolatilization, whereas for the combustion term the grain model will be considered as well. Transport-controlled models are unlikely under our experimental conditions and will not be included in this study. Then, two arrangements, VR/VR and VR/grain (pyrolysis/combustion), will be evaluated.

This paper sets out to check the validity of these kinetic models by obtaining the corresponding apparent kinetic parameters for thermal decomposition of several wood species under N_2–O_2 atmospheres of different molar ratios using non-isothermal thermogravimetric experiments.

EXPERIMENTAL

Four wood species have been investigated, corresponding to holm oak (*Quercus rotundifolia*), cork oak (*Quercus suber*), aleppo pine (*Pinus halepensis*) and eucalyptus (*Eucalyptus rostrata*). The raw materials were used as 65–80 mesh sawdust obtained from single logs of trees from Malaga (S.E. Spain). The aproximate ages of the trees were over 50 years in the cases of holm oak and cork oak, about 40 for aleppo pine and 15–20 years for eucalyptus. The logs were stored at room temperature for a two-month period and, prior to the thermogravimetric experiments, the sawdust samples were dried overnight at 333 K and 10^{-2} Torr.

The TG experiments were carried out in a Thermoflex Rigaku thermobalance, where the weight loss curves were obtained in non-isothermal conditions at linear heating rates of 5, 10 and 20 K min^{-1}. N_2–O_2 gas mixtures with 95/5, 90/10 and 80/20 molar ratios were continuously passed at a 70 ml min^{-1} (STP) flow rate. The initial sample weight was always within the range of 4–4.5 mg. As the thermocouple is self-contained in the sample pan holder, it detects the temperature of the solid, which was assumed to be homogeneous owing to the small thickness of the solid sample.

KINETIC ANALYSIS

The weight loss that a wood sample undergoes when heated in an oxygen-bearing atmosphere can be attributed to volatile matter distillation and to combustion reactions affecting the remaining solid. The relative contribution of these two groups of reactions will be dependent on temperature and on the chemical composition of the actual solid phase. Pyrolysis and combustion can be considered from an overall approach, and the kinetics of weight loss can be expressed by the following general equation

$$-\frac{d\omega}{dt} = k_1(T) f_1(\omega - \omega_1) + k_2(T) f_2(\omega - \omega_2) P_{O_2}^n \quad (1)$$

where ω corresponds to the remaining solid weight at time t, k_1 and k_2 are the temperature-dependent apparent kinetic constants for pyrolysis and combustion, respectively, and ω_1 and ω_2 represent the ultimate non-volatile and non-combustible matter. Oxygen partial pressure is represented by P_{O_2} and n is the apparent reaction order with respect to it, for which a value of 1 is frequently adopted [5,19].

In non-isothermal conditions and using conversion, eqn. (1) can be rewritten as

$$\frac{d\alpha}{dt} = A_{01} \exp(-E_1/RT) f_1(\alpha) + A_{02} \exp(-E_2/RT) f_2(\alpha) P_{O_2}^n \quad (2)$$

where T and t are related through the heating rate (linear in our case). A_{01} and E_1 represent, respectively, the preexponential factor and the apparent activation energy for pyrolysis, A_{02} and E_2 being the corresponding parameters for combustion. Conversion, α, is referred to the ultimate solid residue, namely the non-combustible matter. Thus

$$\alpha = \frac{\omega_0 - \omega}{\omega_0 - \omega_2} \quad (3)$$

where ω_0 is the initial sample weight (dry basis).

The kinetic equation for the VR/VR combination can be expressed by

$$-\frac{d\omega}{dt} = k_1(\omega - \omega_1) + k_2(\omega - \omega_2) P_{O_2} \quad (4)$$

which can be rewritten as

$$\frac{d\alpha}{dt} = k_1 \frac{(\omega - \omega_1)}{(\omega_0 - \omega_2)} + k_2(1 - \alpha) P_{O_2} \quad (5)$$

and easily transformed to the final expression

$$\frac{d\alpha}{dt} = A_{01} \exp(-E_1/RT)(1 - \alpha - a) + A_{02} \exp(-E_2/RT)(1 - \alpha) P_{O_2} \quad (6)$$

where

$$a = \frac{\omega_1 - \omega_2}{\omega_0 - \omega_2} \tag{7}$$

In the case of the VR/grain combination the kinetic equation is given by

$$\frac{d\alpha}{dt} = A_{01} \exp(-E_1/RT)(1 - \alpha - a) + A_{02} \exp(-E_2/RT)(1 - \alpha)^{2/3} P_{O_2} \tag{8}$$

Equations (6) and (8) have been integrated numerically by the fourth-order Runge–Kutta method. In both equations the restriction is made that the pyrolysis term is zero for $\alpha > (1 - a)$ (i.e. $\omega < \omega_1$), although, in any case, its contribution is negligible in such conditions. This restriction derives from the assumption that the non-pyrolysable matter does not undergo combustion until the volatile matter has been removed from the solid (whether by pyrolysis or combustion), which is implicit in the formulation of the general kinetic expression given by eqn. (1). A Marquardt routine was used to optimize the A_{02} and E_2 values leading to the best fit among calculated and experimental $\alpha(t$ or $T)$ values. A_{01} and E_1 were previously determined from pyrolysis experiments carried out in a N_2 atmosphere. Two complementary criteria have been used to check the validity of the kinetic expressions (6) and (8). The sum of the squares of residuals and the comparison of the best-fitting values resulting for the kinetic parameters at the three different heating rates used ($\beta = 5$, 10 and 20 K min^{-1}). As these β values fall within a range sufficiently narrow for us to assume that the chemistry of the process is scarcely affected, a model which provides an adequate description of the problem should lead to similar values of the kinetic parameters at the three heating rates.

RESULTS AND DISCUSSION

Thermal decomposition in inert atmosphere

Prior to studying the kinetics of wood thermal decomposition in oxygen-bearing atmospheres, we obtained the kinetic parameters corresponding to pyrolysis in inert (N_2) atmosphere. These will be used as the A_{01} and E_1 values in equations (6) and (8). They have been derived from the expression

$$\frac{d\alpha_1}{dt} = A_{01} \exp(-E_1/RT)(1 - \alpha_1) \tag{9}$$

where

$$\alpha_1 = \frac{\omega_0 - \omega}{\omega_0 - \omega_1} \tag{10}$$

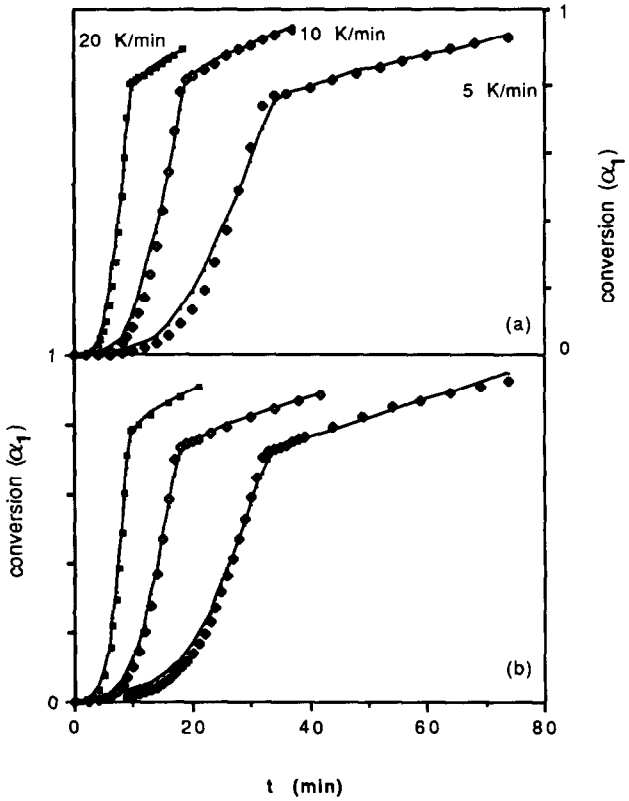

Fig. 1. Experimental $\alpha_1(t)$ curves and calculated points for cork oak (a) and aleppo pine (b) wood thermal decomposition in inert atmosphere.

The experimental weight loss curves corresponding to cork oak and aleppo pine wood in a N_2 atmosphere are shown in Fig. 1, which includes also the calculated $\alpha_1(t)$ values for comparison. Analogous curves were obtained for the two other wood species. For the sake of clarity the curves are presented as α–t plots. They can be easily transformed to α–T plots using the relationship $T = T_0 + \beta t$ where T_0 was always taken as 453 K.

When we used single values of A_{01} and E_1 throughout the entire conversion range, the experimental and calculated $\alpha_1(t)$ values showed significant discrepancies in the conversion region above 0.6–0.7. Thus, a two-stage approach was used to analyse the weight loss curves [20] in which the conversion value corresponding to the breakpoint was optimized by iterations. Table 1 reports the results obtained. For each wood species, the values of the apparent activation energy obtained at different heating rates are very close, and the same can be said for the preexponential factor. As can be seen, substantially smaller values are always obtained in the conversion region corresponding to the second stage. The sum of the squares of residuals shows fairly good values with regard to the number of points

TABLE 1

Apparent kinetic parameters obtained for thermal decomposition of wood in inert atmosphere using the VR model: A_{01} (s^{-1}), E_1 (kJ mol^{-1})

Wood	β (K min^{-1})	Value of α_1 at the breakpoint	First stage		Second stage		Sum of the squares of residuals	Number of points
			A_{01}	E_1	A_{01}	E_1		
Eucalyptus	5	0.570	1.14×10^{6}	101.8	2.07×10^{-3}	12.5	0.0509	65
	10	0.610	1.14×10^{6}	101.2	3.77×10^{-3}	12.2	0.0303	58
	20	0.640	1.20×10^{6}	98.6	8.00×10^{-3}	12.1	0.0210	43
Holm oak	5	0.703	1.13×10^{5}	89.5	6.08×10^{-3}	18.9	0.0348	30
	10	0.752	1.10×10^{5}	88.6	1.01×10^{-2}	17.4	0.0270	32
	20	0.782	1.58×10^{5}	87.8	2.75×10^{-2}	19.7	0.0116	23
Cork oak	5	0.743	2.42×10^{5}	92.6	9.46×10^{-3}	18.1	0.0186	28
	10	0.794	2.95×10^{5}	92.7	2.41×10^{-2}	18.5	0.0197	25
	20	0.783	3.67×10^{5}	91.4	1.58×10^{-2}	16.1	0.0185	26
Aleppo pine	5	0.719	1.45×10^{5}	90.1	1.97×10^{-3}	7.9	0.0153	40
	10	0.734	2.15×10^{5}	90.5	1.96×10^{-3}	7.5	0.0055	25
	20	0.777	3.59×10^{5}	90.9	3.94×10^{-3}	7.1	0.0042	20

TABLE 2

Apparent kinetic parameters obtained for thermal decomposition of eucalyptus wood in oxygen-bearing atmospheres using the VR/VR (pyrolysis/combustion) model: A_{02} (s^{-1} atm^{-1}), E_2 (kJ mol^{-1})

O_2 (mol%)	β (K min^{-1})	Value at α at the breakpoint	First stage		Second stage		Sum of the squares of residuals	Number of points
			A_{02}	E_2	A_{02}	E_2		
5	5	0.48	1.02×10^6	92.0	1.25×10^3	68.4	0.00754	32
	10	0.47	1.00×10^6	88.5	1.28×10^3	64.8	0.01061	32
	20	0.49	6.73×10^5	86.0	1.44×10^3	62.6	0.00446	22
10	5	0.49	1.09×10^6	92.4	1.34×10^3	68.4	0.00913	29
	10	0.48	1.10×10^6	93.4	2.10×10^3	69.6	0.00934	31
	20	0.48	9.48×10^5	92.8	2.09×10^3	68.6	0.01270	32
20	5	0.48	8.42×10^5	91.2	1.03×10^3	69.4	0.00737	41
	10	0.52	1.14×10^6	91.9	1.34×10^3	69.4	0.00790	34
	20	0.49	1.15×10^6	93.2	1.90×10^3	70.3	0.00960	32
Average			9.96×10^5 (11.7) [a]	91.3 (2.4)	1.53×10^3 (21.8)	67.9 (2.8)		

[a] The figure in parentheses is the mean relative deviation (%).

TABLE 3

Apparent kinetic parameters obtained for thermal decomposition of eucalyptus wood in oxygen-bearing atmospheres using the VR/grain (pyrolysis/combustion) model: A_{02} (s^{-1} atm^{-1}), E_2 (kJ mol^{-1})

O_2 (mol%)	β (K min^{-1})	Value of α at the breakpoint	First stage		Second stage		Sum of the squares of residuals	Number of points
			A_{02}	E_2	A_{02}	E_2		
5	5	0.48	3.31×10^5	101.1	6.13 [a]	57.3	0.00954	32
	10	0.47	2.00×10^6	91.6	804	64.7	0.01200	32
	20	0.49	5.40×10^5	85.2	962	63.3	0.00534	22
10	5	0.49	1.20×10^6	92.8	750	67.7	0.00925	29
	10	0.48	1.71×10^6	93.0	871	67.1	0.01020	31
	20	0.48	6.42×10^5	90.7	1404	68.9	0.00981	32
20	5	0.48	5.93×10^5	89.9	163	61.7	0.00746	41
	10	0.52	1.95×10^6	94.6	384	64.9	0.00992	34
	20	0.49	1.26×10^6	94.2	995	69.4	0.00738	32
Average			1.14×10^6 (47.5) [b]	$E_2 = 92.8$ (3.1)	704.3 (34.1)	65.0 (4.48)		

[a] Excluded from average.

[b] The figure in parentheses is the mean relative deviation (%).

considered in each case. The highest mean relative deviation was 3%. Thus, the validity of the VR model to describe the pyrolysis step can be assumed under our experimental conditions.

Thermal decomposition in oxidizing atmosphere

Using the A_{01} and E_1 values previously obtained, we have determined the kinetic parameters corresponding to the combustion step (A_{02} and E_2) by fitting the experimental weight loss curves in oxygen-bearing atmospheres to eqns. (6) and (8) which, as indicated before, correspond, respectively, to the VR/VR and VR/grain (pyrolysis/combustion) arrangements. Again, a two-stage analysis was used because a good reproduction of the experimental α–t curves was not possible when using single values of A_{02} and E_2 throughout the entire conversion range. The A_{01} and E_1 values used before and after the conversion value corresponding to the breakpoint were now those reported in Table 1 for the first and second stages, respectively. The situation described in the following discussion is applicable to all the experiments performed, although for the sake of simplicity we are presenting a representative selection of the results obtained.

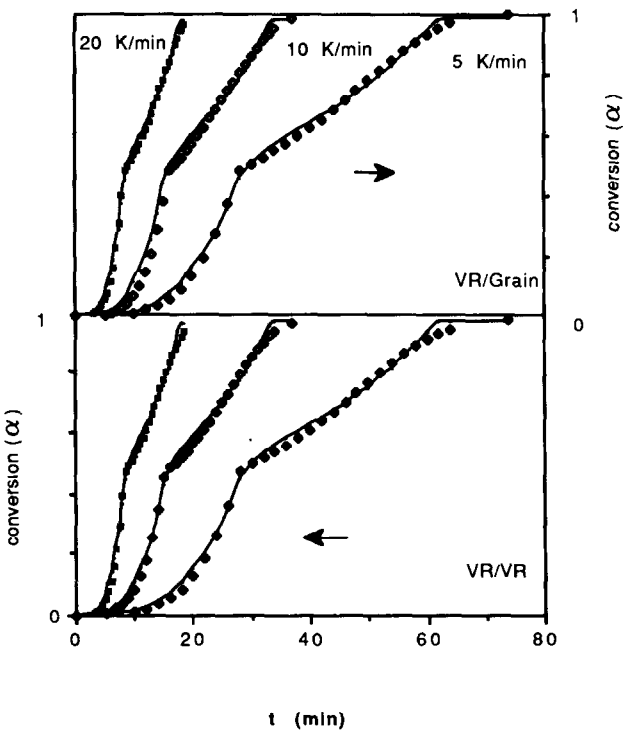

Fig. 2. Experimental $\alpha(t)$ curves and calculated points for eucalyptus wood thermal decomposition in 10% O_2 atmosphere.

TABLE 4

Apparent kinetic parameters obtained from the joint treatment of data obtained at three heating rates for eucalyptus wood thermal decomposition in oxygen-bearing atmospheres: A_{02} (s^{-1} atm^{-1}), E_2 (kJ mol^{-1})

Model	O_2 (mol%)	Value of α at the breakpoint	First stage		Second stage		Sum of the squares of residuals	Number of points
			A_{02}	E_2	A_{02}	E_2		
VR/VR	5	0.48	9.37×10^5	92.45	3850	75.61	0.4438	189
	10	0.48	1.85×10^6	94.71	2983	71.59	0.1591	195
	20	0.48	2.28×10^6	92.23	7754	75.66	0.1614	195
VR/grain	5	0.48	2.02×10^6	96.02	8396	83.39	0.4751	189
	10	0.48	2.11×10^6	92.34	1506	68.85	0.1992	195
	20	0.48	2.25×10^6	95.72	5351	77.61	0.1633	195

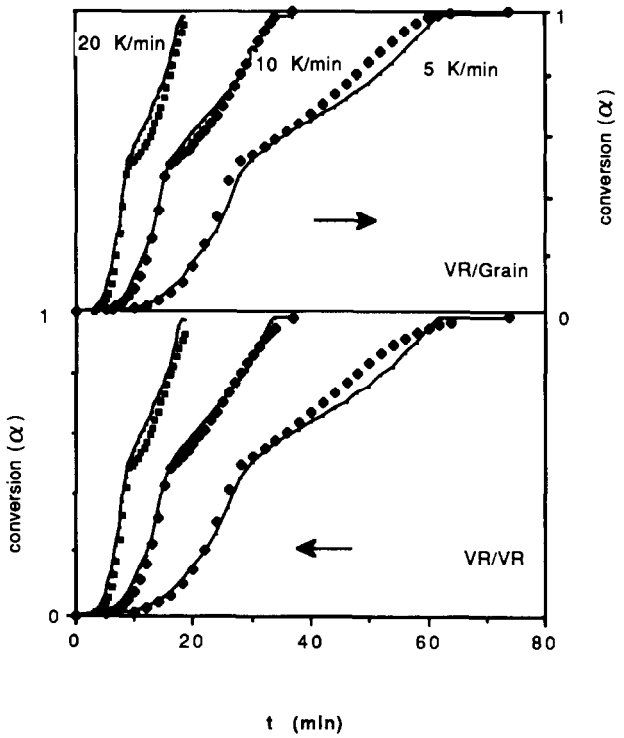

Fig. 3. Experimental $\alpha(t)$ curves and calculated points using the kinetic parameters determined from the joint treatment of data obtained at three different heating rates for eucalyptus wood in 10% O_2 atmosphere.

Tables 2 and 3 show the results obtained for eucalyptus wood at different heating rates and oxygen concentrations. As can be seen from the sum of the squares of residuals, it becomes very difficult to discriminate between the two models investigated, as both lead to very similar values. Looking at the A_{02} and E_2 values obtained at different heating rates for each oxygen concentration, the VR/VR configuration shows a better behaviour than the VR/grain. Nevertheless, it can be said that both provide a fairly accurate description of the experimental weight loss curces. As an example, Fig. 2 shows the experimental α–t curves obtained in 10% molar oxygen atmosphere together with the $\alpha(t)$ values calculated from the two kinetic equations evaluated, using the values of the kinetic parameters reported in Tables 2 and 3.

A further discrimination of the two kinetic equations was attempted by fitting in each case all the data obtained from the three temperature-programmed runs performed at a different heating rate as a way to overcome the problem derived from the interrelation of α and $T(t)$ [11]. Table 4 reports the values of the apparent kinetic parameters obtained in this way for eucalyptus wood, and Fig. 3 shows the $\alpha(t)$ values calculated by using

TABLE 5

Apparent kinetic parameters obtained for thermal decomposition of holm oak wood in oxygen-bearing atmospheres using the VR/VR model: A_{02} (s^{-1} atm^{-1}), E_2 (kJ mol^{-1})

O_2 (mol%)	β (K min^{-1})	Value of α at the breakpoint	First stage		Second stage		Sum of the squares of residuals	Number of points
			A_{02}	E_2	A_{02}	E_2		
5	5	0.628	3.46×10^5	82.6	4.2×10^4	80.5	0.0070	28
	10	0.610	3.55×10^5	80.7	5.5×10^4	80.0	0.0079	28
	20	0.635	3.10×10^5	80.2	4.52×10^4	80.3	0.0069	22
10	5	0.647	3.74×10^5	85.3	7.68×10^4	87.5	0.0072	26
	10	0.627	3.97×10^5	83.8	8.49×10^4	86.1	0.0096	30
	20	0.613	3.60×10^5	83.5	8.76×10^4	84.7	0.0112	28
20	5	0.583	3.72×10^5	88.1	1.81×10^4	83.9	0.0089	35
	10	0.590	3.96×10^5	89.6	1.85×10^4	82.5	0.0093	28
	20	0.630	3.92×10^5	85.2	2.5×10^4	80.3	0.0025	24
Average			3.67×10^5 (5.8) [a]	84.3 (2.9)	5.03×10^4 (46.1)	82.9 (2.9)		

[a] The figure in parentheses is the mean relative deviation (%).

TABLE 6

Apparent kinetic parameters obtained for thermal decomposition of cork oak wood in oxygen-bearing atmospheres using the VR/VR model: A_{02} (s^{-1} atm^{-1}), E_2 (kJ mol^{-1})

O_2 (mol%)	β (K min^{-1})	Value of α at the breakpoint	First stage		Second stage		Sum of the squares of residuals	Number of points
			A_{02}	E_2	A_{02}	E_2		
5	5	0.658	2.73×10^5	81.6	1.06×10^5	86.6	0.0089	27
	10	0.600	3.07×10^5	80.4	1.29×10^5	85.3	0.0106	28
	20	0.665	2.70×10^5	79.5	1.35×10^5	85.6	0.0084	29
10	5	0.645	2.35×10^5	83.2	5.39×10^4	87.8	0.0073	25
	10	0.634	3.34×10^5	83.6	9.01×10^4	87.7	0.0051	26
	20	0.650	3.40×10^5	83.1	8.10×10^4	83.4	0.0066	28
20	5	0.657	2.77×10^5	86.4	3.51×10^4	86.2	0.0029	24
	10	0.650	3.28×10^5	85.3	6.54×10^4	87.8	0.0061	23
	20	0.665	3.82×10^5	84.6	7.65×10^4	84.5	0.0105	22
Average			3.05×10^5 (12.1) [a]	83.1 (2.0)	8.58×10^4 (30.3)	86.1 (1.4)		

[a] The figure in parentheses is the mean relative deviation (%).

TABLE 7

Apparent kinetic parameters obtained for thermal decomposition of aleppo pine wood in oxygen-bearing atmospheres using the VR/VR model: A_{02} (s^{-1} atm^{-1}), E_2 (kJ mol^{-1})

O_2 (mol%)	β (K min^{-1})	Value of α at the breakpoint	First stage		Second stage		Sum of the square of residuals	Number of points
			A_{02}	E_2	A_{02}	E_2		
5	5	0.580	8.04×10^4	79.5	2.25×10^4	80.5	0.0142	29
	10	0.583	1.09×10^5	80.7	3.07×10^4	79.7	0.0065	29
	20	0.590	1.00×10^5	87.5	2.83×10^4	78.8	0.0085	30
10	5	0.590	8.25×10^4	82.3	4.03×10^4	85.9	0.0060	25
	10	0.600	8.00×10^4	80.4	4.82×10^4	84.0	0.0073	28
	20	0.602	9.32×10^4	83.0	4.00×10^4	82.2	0.0097	30
20	5	0.570	8.18×10^4	83.6	3.37×10^4	87.4	0.0070	34
	10	0.592	1.00×10^5	83.4	4.94×10^4	85.5	0.0084	25
	20	0.594	9.88×10^4	83.0	5.00×10^4	81.9	0.0181	22
Average			9.17×10^4 (10.2) [a]	82.6 (2.0)	3.81×10^4 (21.8)	82.9 (3.0)		

[a] The figure in parentheses is the mean relative deviation (%).

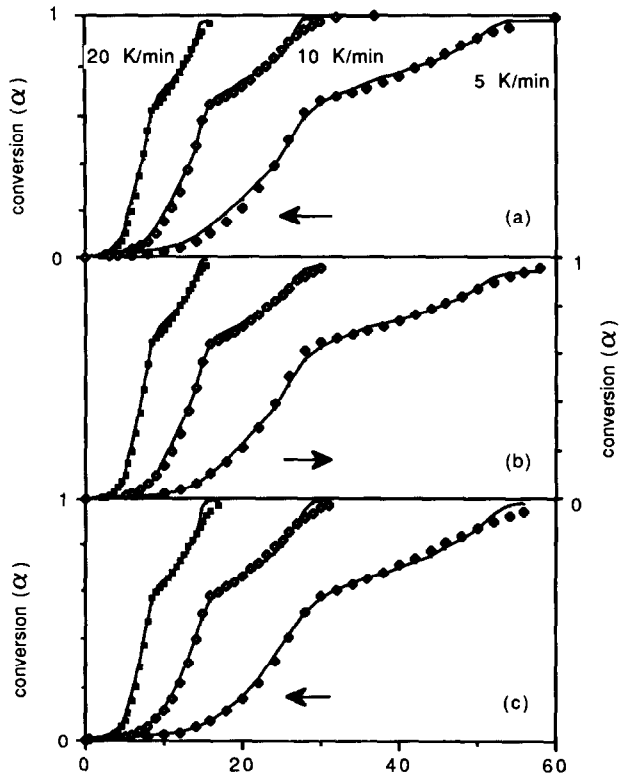

Fig. 4. Experimental $\alpha(t)$ curves and calculated points for holm oak (a), cork oak (b) and aleppo pine (c) wood thermal decomposition in 10% O_2 atmosphere, VR/VR model.

these parameters from the VR/VR and VR/grain combinations, respectively. As can be seen, the reproduction of the experimental curves is now poorer than that obtained from the treatment of the kinetic data at each heating rate individually, but it allows a better discrimination between the models investigated, the VR/VR model being somewhat more reliable.

The kinetic parameters obtained for the three other wood species investigated as derived from the VR/VR combination, are represented in Tables 5–7. Again, it can be seen that the values obtained at different heating rates are fairly close in each case. The sum of the squares of residuals reveals also the validity of the model to describe the experimental weight loss curves. As an example, Fig. 4 shows the experimental and calculated $\alpha(t)$ values in 10% O_2 atmosphere.

When comparing the results obtained for the four wood species investigated, a notable difference among the values of the apparent kinetic parameters derived for eucalyptus and those obtained for the three other woods can be observed. Moreover, whereas these last show quite similar values of the apparent activation energy for the first and second stages, eucalyptus does not. Also, it is significant to note that the conversion values at the break-

TABLE 8

Values of the apparent kinetic constant, $k_2 \times 10^4$ (s^{-1} atm^{-1}), at different temperatures

	T (K)	Eucalyptus	Aleppo pine	Holm oak	Cork oak
First stage	520	6.7	4.6	12.5	13.7
	550	21.3	13.1	36.2	39.1
	580	59.7	33.4	93.9	100.1
Second stage	650	53.5	83.0	109.6	103.4
	700	131.2	248.3	327.8	322.6
	750	285.6	641.7	847.2	865.0

point delimiting the first and the second stages are always smaller in the case of eucalyptus. The values of the apparent kinetic constants calculated at representative temperatures from the Arrhenius equation using mean values of E_2 and A_{02} (Table 8) indicate a lower reactivity of aleppo pine wood as compared with the three others within the first stage, whereas in the second stage eucalyptus becomes the least reactive species. Holm oak and cork oak, which belong to the same genus, always show very close values.

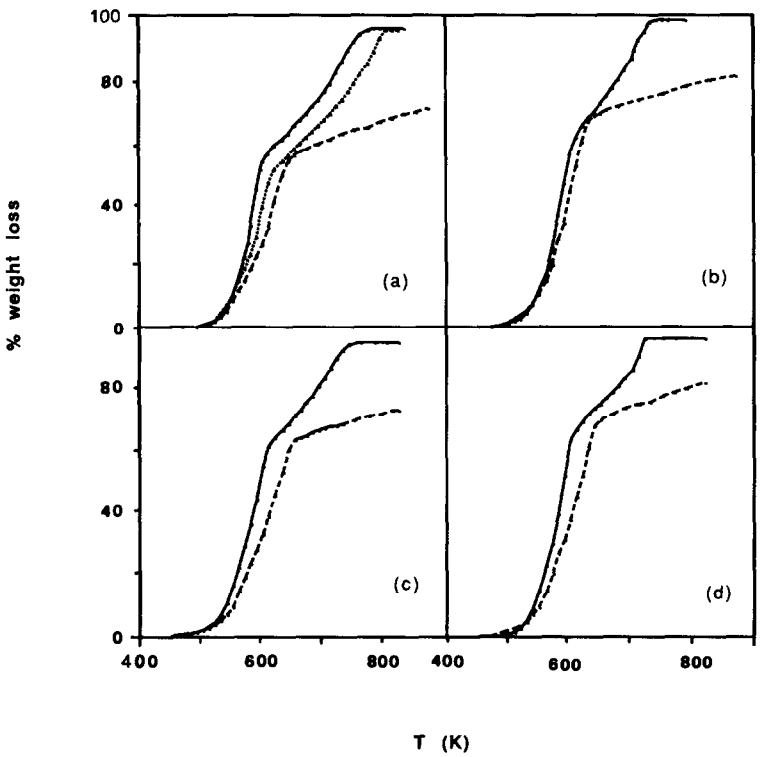

Fig. 5. TGA curves for eucalyptus (a), aleppo pine (b), holm oak (c) and cork oak (d) in N_2 (– – –) and 20% O_2 (———) atmosphere. For eucalyptus, the curve in 5% O_2 (· · · · · ·) is also included.

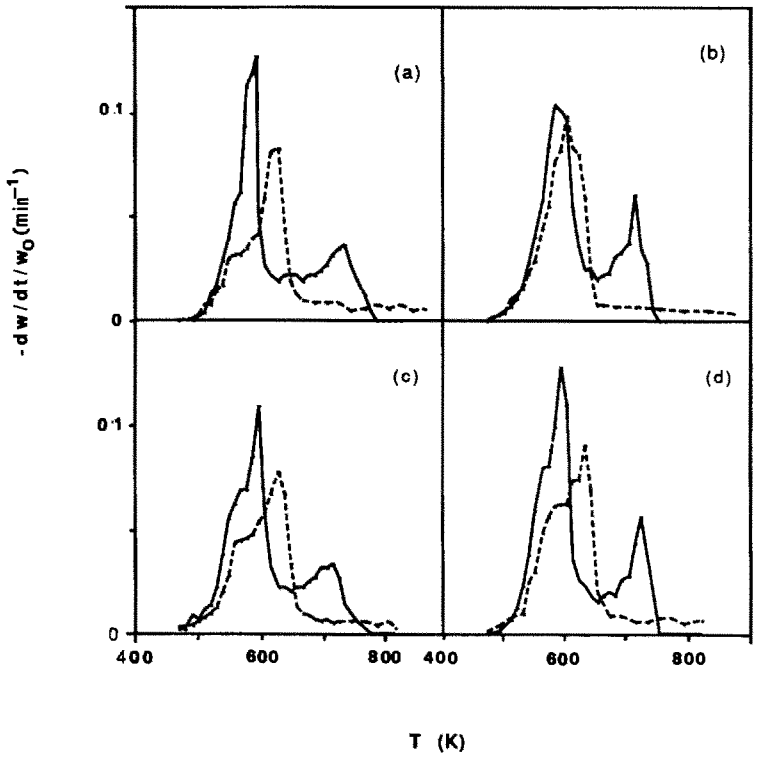

Fig. 6. DTG curves for eucalyptus (a), aleppo pine (b), holm oak (c) and cork oak (d) in N_2 (– – –) and 20% O_2 (———) atmosphere.

With regard to the first and second stages that we have considered in the thermal decomposition of wood, a comparison of the TGA and DTG curves obtained in inert and oxidizing atmospheres (Figs. 5 and 6 respectively) reveals that, in presence of oxygen, two regions can be distinguished within the first stage. In the initial one, up to about 550–560 K or 10% weight loss, devolatilization is practically the sole significant process taking place, whereas, as the temperature increases, the contribution of combustion of the remaining solid becomes more evident. Nevertheless, the substantially smaller influence of oxygen throughout the first stage in the case of aleppo pine is noticeable. In the second stage, combustion represents the major contribution in all the cases. The influence of oxygen concentration can be seen in Fig. 5a, where the TGA curve in 5% molar O_2 has been also included.

The general shape of the DTG curves becomes quite similar, always showing a displacement of the first peak to lower temperatures as well as the presence of a second one around the 700–750 K region in an oxidizing atmosphere.

ACKNOWLEDGEMENT

The authors thank CAICYT for financial support for this research through Project AG-9/82 within the Agroenergetics R&D Programme.

REFERENCES

1 C. Fairbridge and R.A. Ross, Wood Sci. Technol., 12 (1978) 169.
2 C. Vovelle, H. Mellottee and R. Delbourgo, Colloq. Int. Berthelot–Vieille–Mallard–Le Chatelier, [Actes], 1st, University of Bordeaux I, 1981, Vol. 2, p. 580.
3 J.R. Richard and C. Vovelle, Comm. Eur. Communities, [Rep.] EUR 10024, 1985, p. 895.
4 R.G. Jenkins, S.P. Nandi and P.L. Walker, Fuel, 52 (1973) 288.
5 S. Dutta and C.Y. Wen, Ind. Eng. Chem. Process Des. Dev., 16 (1977) 31.
6 J.L. Su and D.D. Perlmutter, AIChE J., 31 (1985) 973.
7 L.R. Radovic, P.L. Walker and R.G. Jenkins, Fuel, 62 (1983) 209.
8 G. Ballal and K. Zygourakis, Chem. Eng. Commun., 49 (1986) 181.
9 M. Rostam-Abadi, D.L. Moran and J.A. De Barr, Prepr. Pap. Am. Chem. Soc. Div. Fuel Chem., 33 (4) (1988) 862.
10 J.K. Floess, J.P. Longwell and A.F. Sarofim, Energy Fuels, 2 (1988) 18.
11 K. Miura and P.L. Silverston, Energy Fuels, 3 (1989) 243.
12 P.A. Ramanchandran and L.K. Doraiswamy, AIChE J., 28 (1982) 881.
13 S.K. Bathia and D.D. Perlmutter, AIChE J., 26 (1980) 379.
14 G.R. Gavalas, AIChE. J., 26 (1980) 577.
15 J.L. Su and D.D. Perlmutter, AIChE J., 30 (1984) 967.
16 S. Reyes and K.F. Jensen, Chem. Eng. Sci., 41 (1986) 333.
17 G. Ballal and K. Zygourakis, Ind. Eng. Chem. Res., 26 (1987) 211.
18 T. Cordero, F. García and J.J. Rodríguez, Thermochim. Acta, 149 (1989) 225.
19 P.L. Walker, L. Ruskino and L.G. Austin, Adv. Catal., 11 (1959) 133.
20 T. Cordero, J.M. Rodríguez-Maroto, J. Rodríguez-Mirasol and J.J. Rodríguez, Thermochim. Acta, 164 (1990) 135.